Topology and geometry under nonlinear electromagnetic spotlight: An experimental perspective II

Light-matter interactions

Qiong Ma
Physics Department
Boston College

Intrinsic photocurrent generation

Extrinsic
(P-N junction)

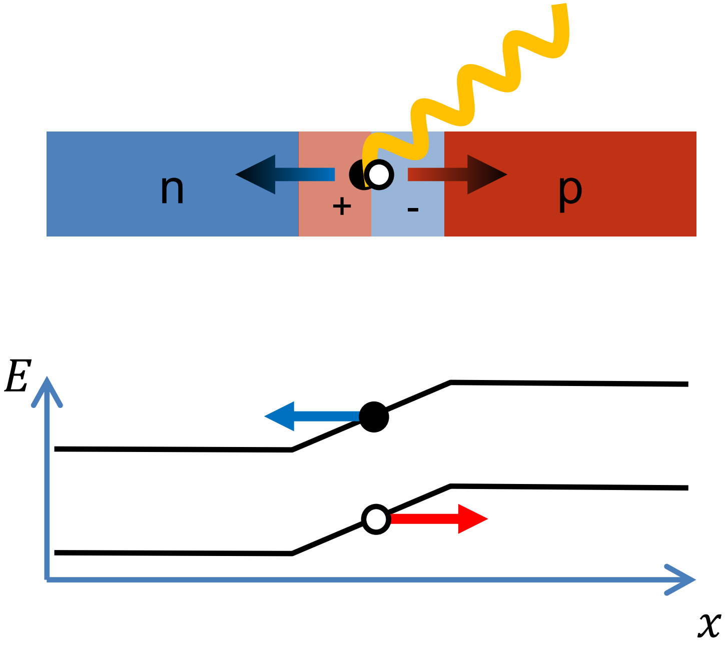

Intrinsic
(bulk photovoltaic effect)

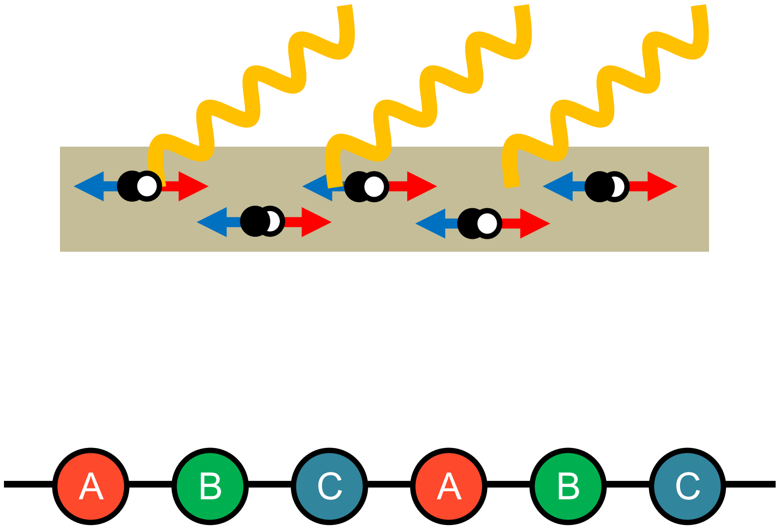

Intrinsic photocurrent generation – second-order response

$$A_i = A_0 + \underbrace{\alpha_{ij}E_j}_{\text{Linear response}} + \underbrace{\chi^{(2)}_{ijk}E_iE_j}_{\text{Second-order response}} + \cdots$$

Second-harmonic generation (SHG)

$\omega \Rightarrow \omega + \omega$

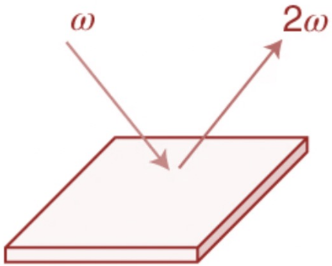

$$P_i^{2\omega} = \chi^{(2)}_{ijk}E_j^{\omega}E_k^{\omega}$$

Photocurrent generation (PC)

$\omega \Rightarrow \omega - \omega$

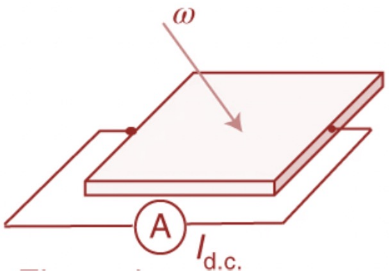

$$I_i^{0\omega} = \chi^{(2)}_{ijk}E_j^{\omega}E_k^{\omega}$$

Intrinsic photocurrent: a broadband approach

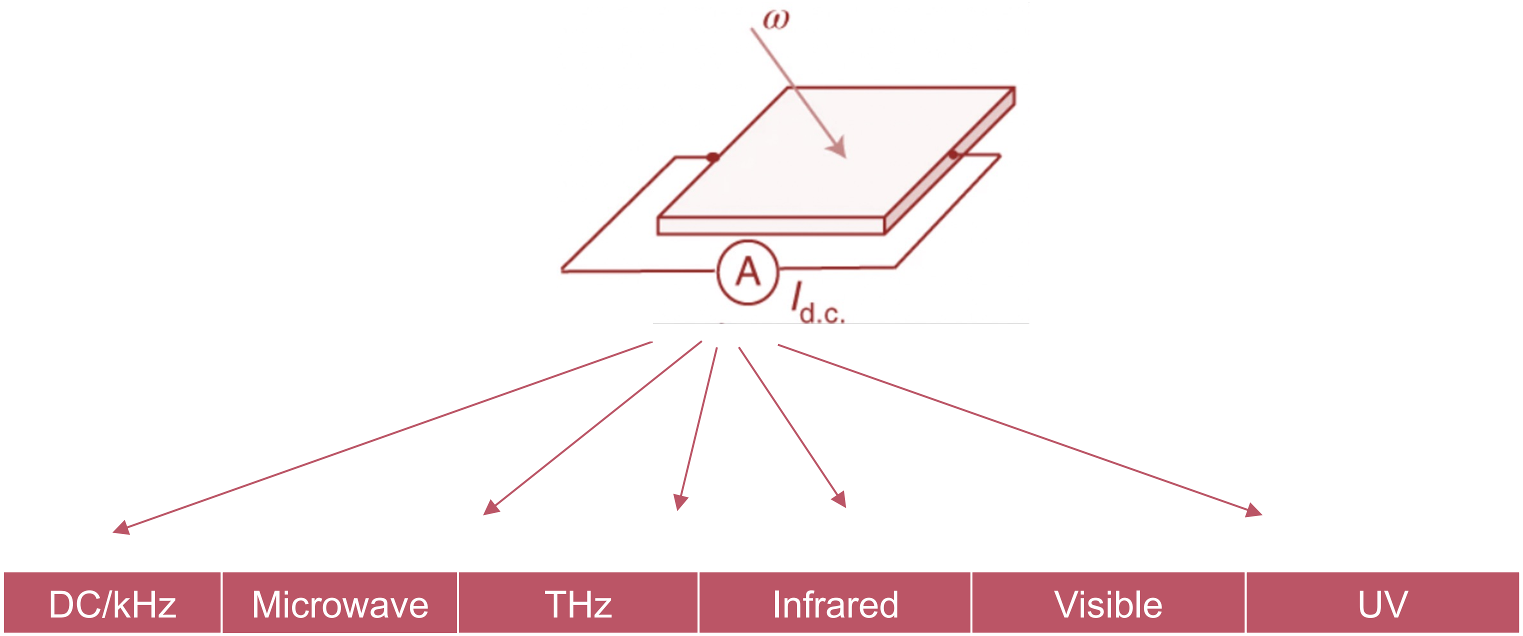

Ma, et al., Nature Materials 20, 1601 (2021) Review article

Different mechanisms for intrinsic photocurrent

Time-reversal symmetric

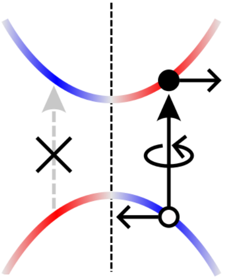

injection current

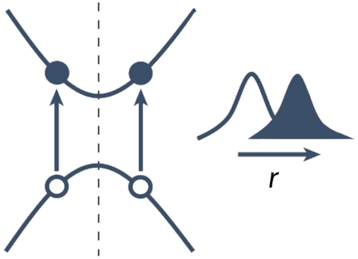

shift current

Time-reversal breaking

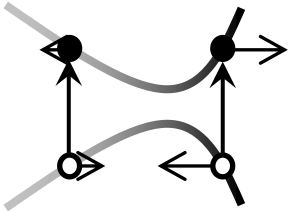

linear injection current

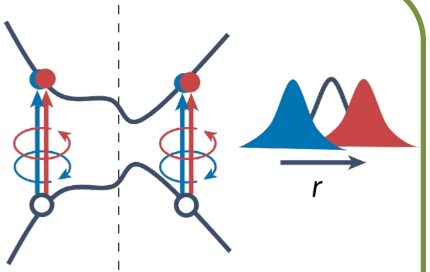

circular shift current

Outline

- Intrinsic photocurrents in WTe_2
- Intrinsic photocurrents in inversion-breaking Weyl
- Intrinsic photocurrents and emergent chirality
- Outlook

Outline

- Intrinsic photocurrents in WTe_2
- Intrinsic photocurrents in inversion-breaking Weyl
- Intrinsic photocurrents and emergent chirality
- Outlook

Berry curvature dipole effect

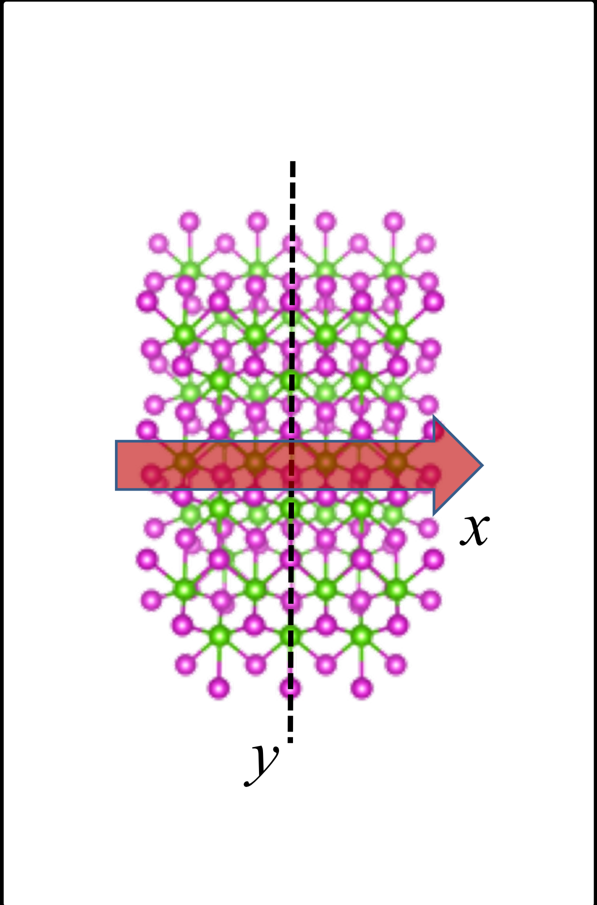

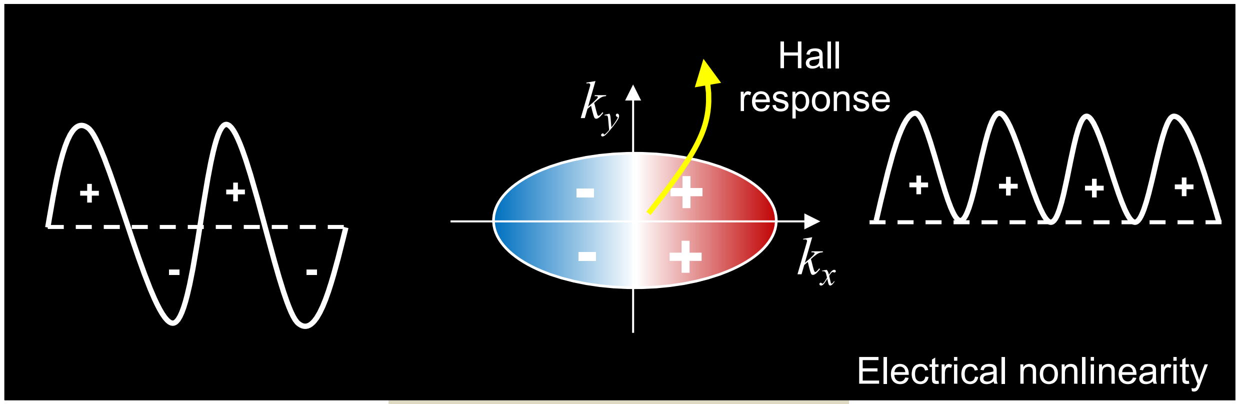

Berry curvature dipole

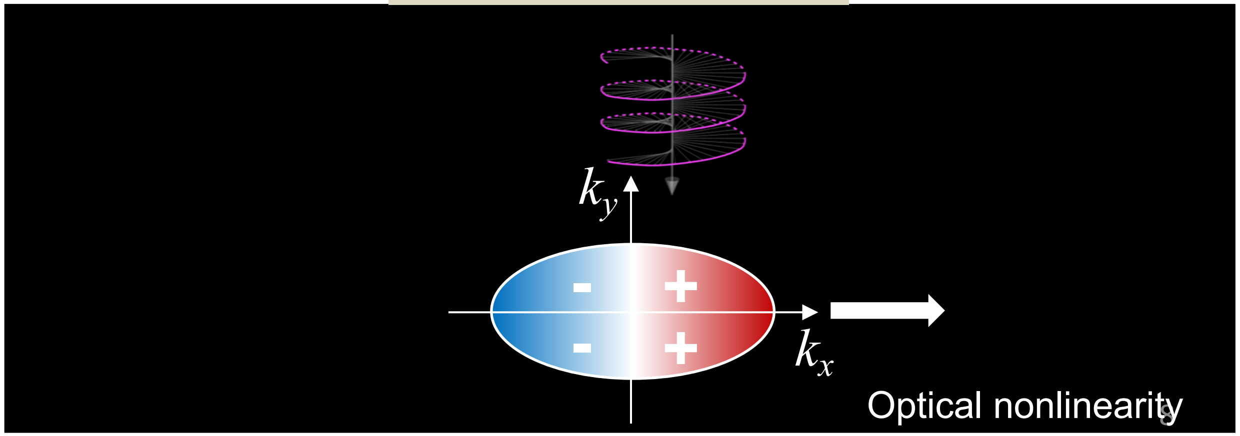

Berry curvature and optical chiral selection

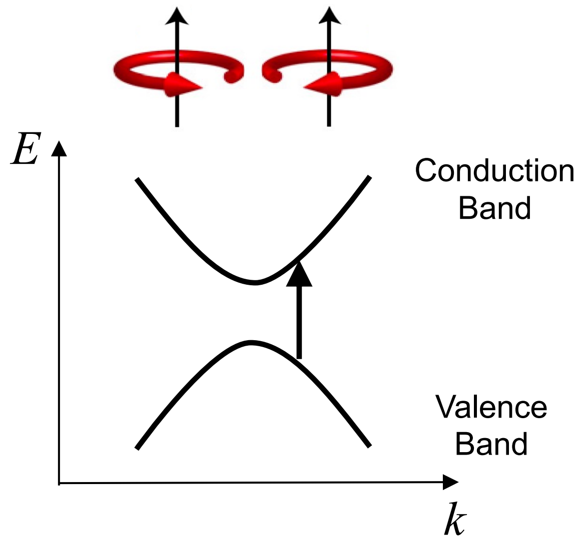

$$|\mathcal{P}^{\mathrm{RCP}}(\vec{k})|^2 - |\mathcal{P}^{\mathrm{LCP}}(\vec{k})|^2 \propto \Omega(\vec{k})$$

Xiao, Chang, Niu, RMP (2010)

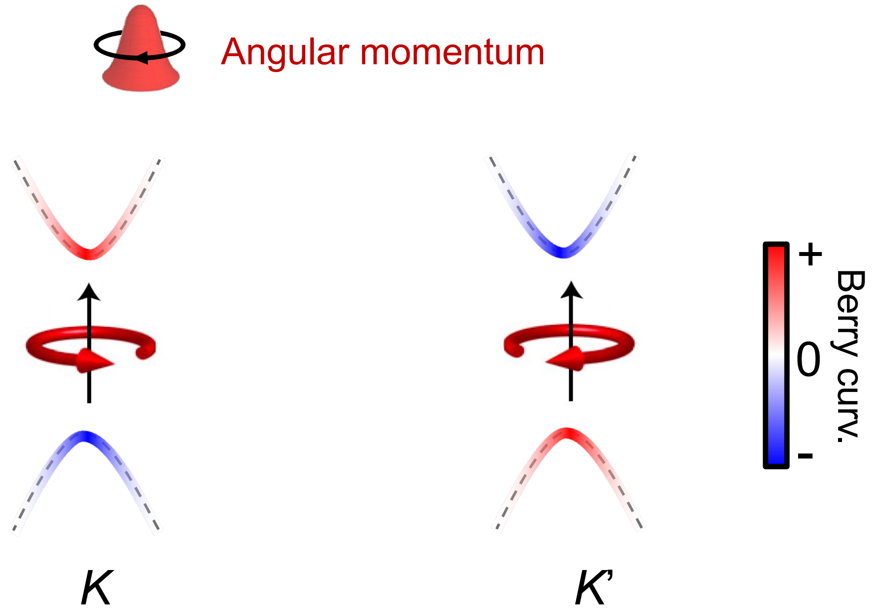

Gapped graphene,
Semiconducting TMD monolayers

Intraband and interband Berry curvature dipole

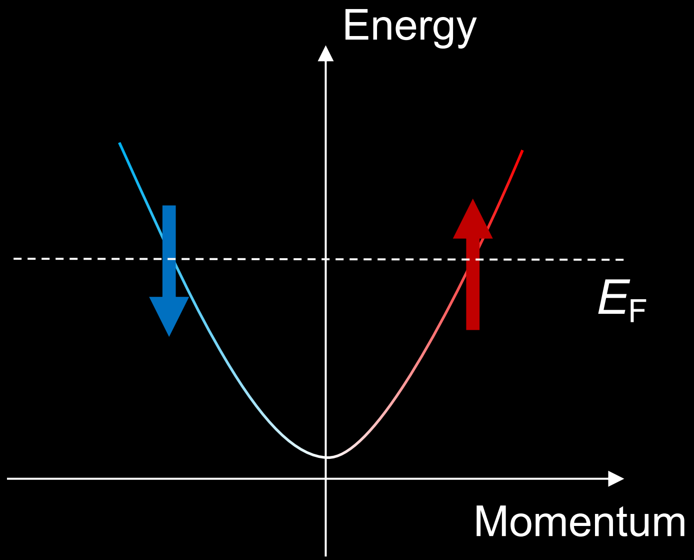

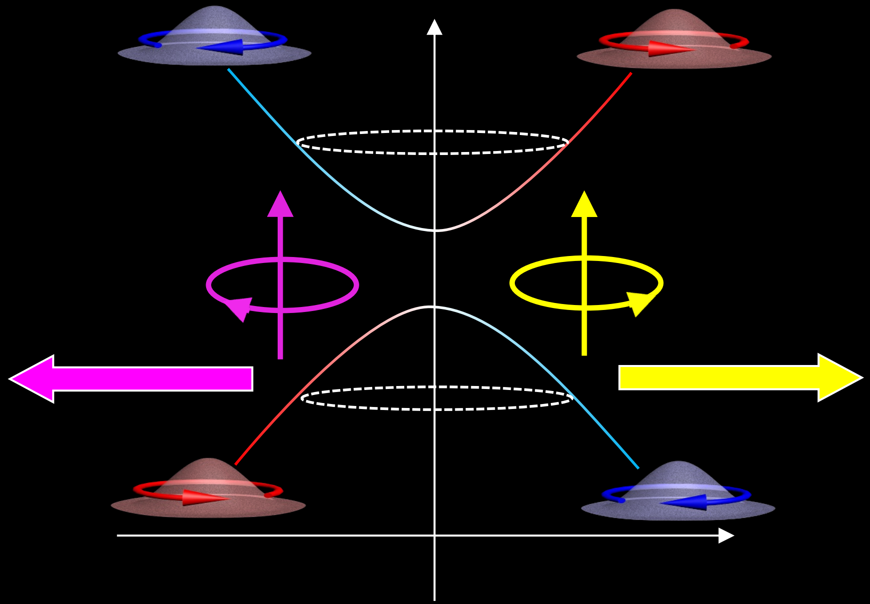

$$\boldsymbol{\Lambda} = \int d^2k\, f(\boldsymbol{k}) \nabla_{\boldsymbol{k}} \Omega_z(\boldsymbol{k})$$

$$\boldsymbol{\Lambda} = \oint d\boldsymbol{k} \times \boldsymbol{\Omega}(\boldsymbol{k})$$

Nature **565**, 337–342 (2019); Nature Physics 14, 900 (2018)

Circular photogalvanic effect (CPGE)

Dipole distribution of Berry curvature

+

Optical selection rules

$$I_i^{0\omega} = \chi_{ijk}^{(2)} E_j^{\omega} E_k^{\omega}$$

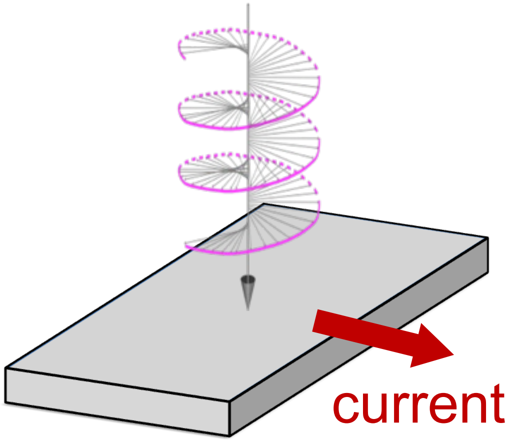

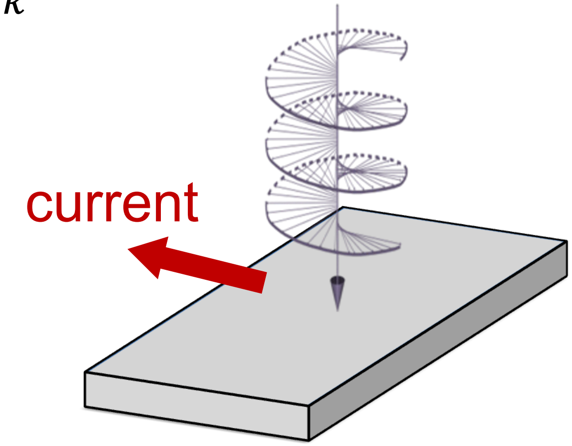

Scanning Photocurrent Microscopy

Electrical current driven solely by the light

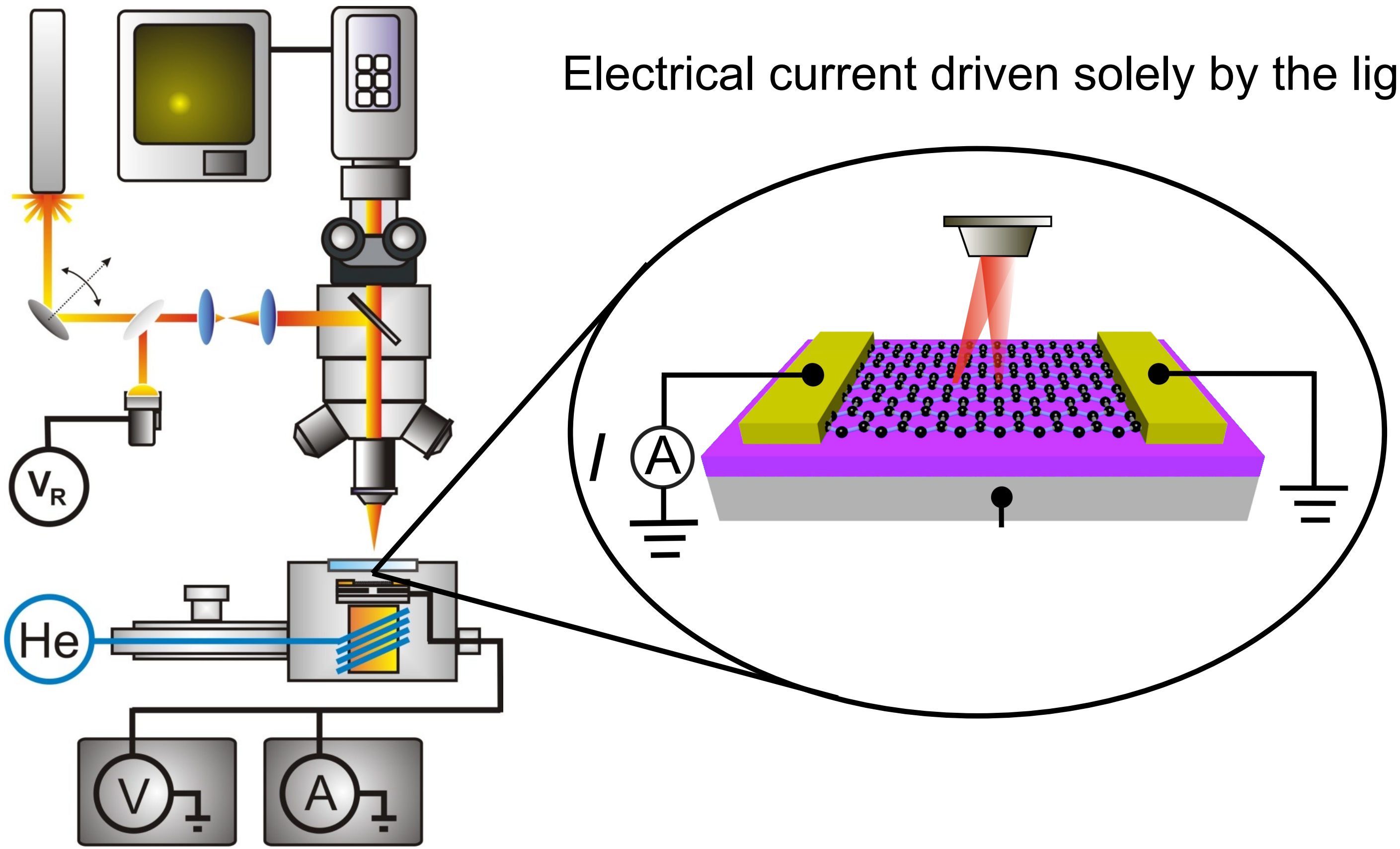

*Inter*band Berry curvature dipole and CPGE

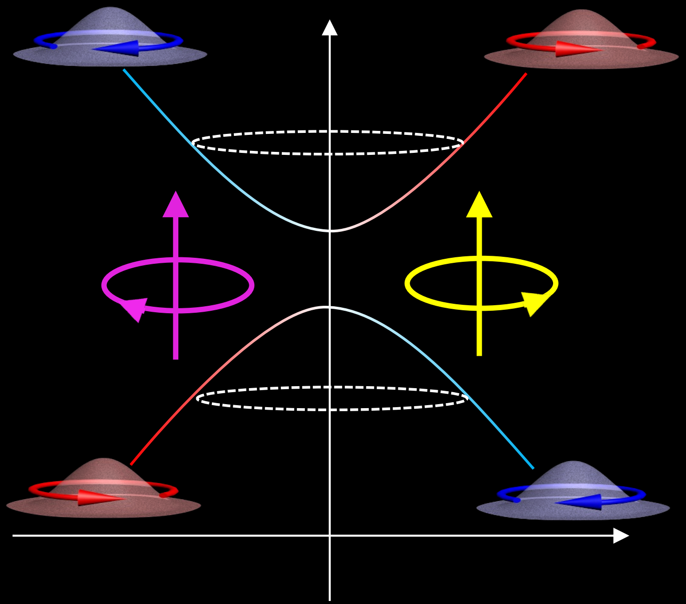

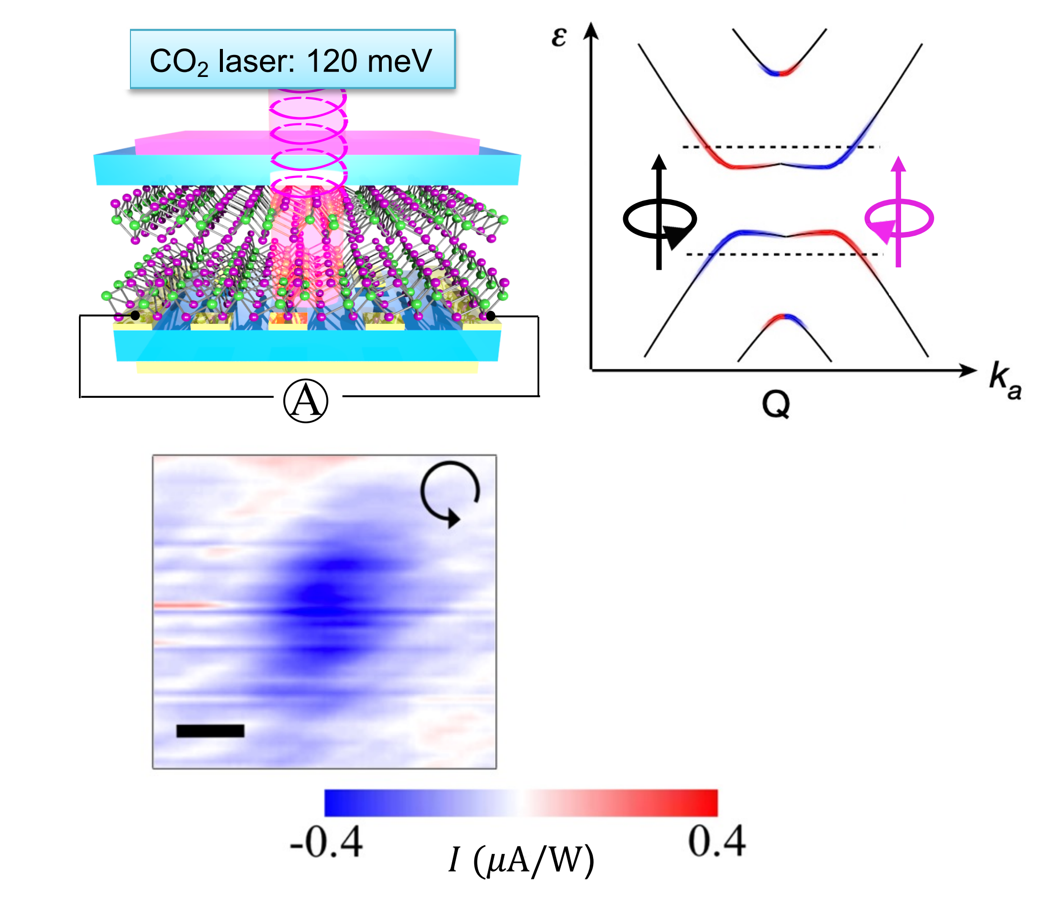

Photocurrent in graphene with broken symmetry

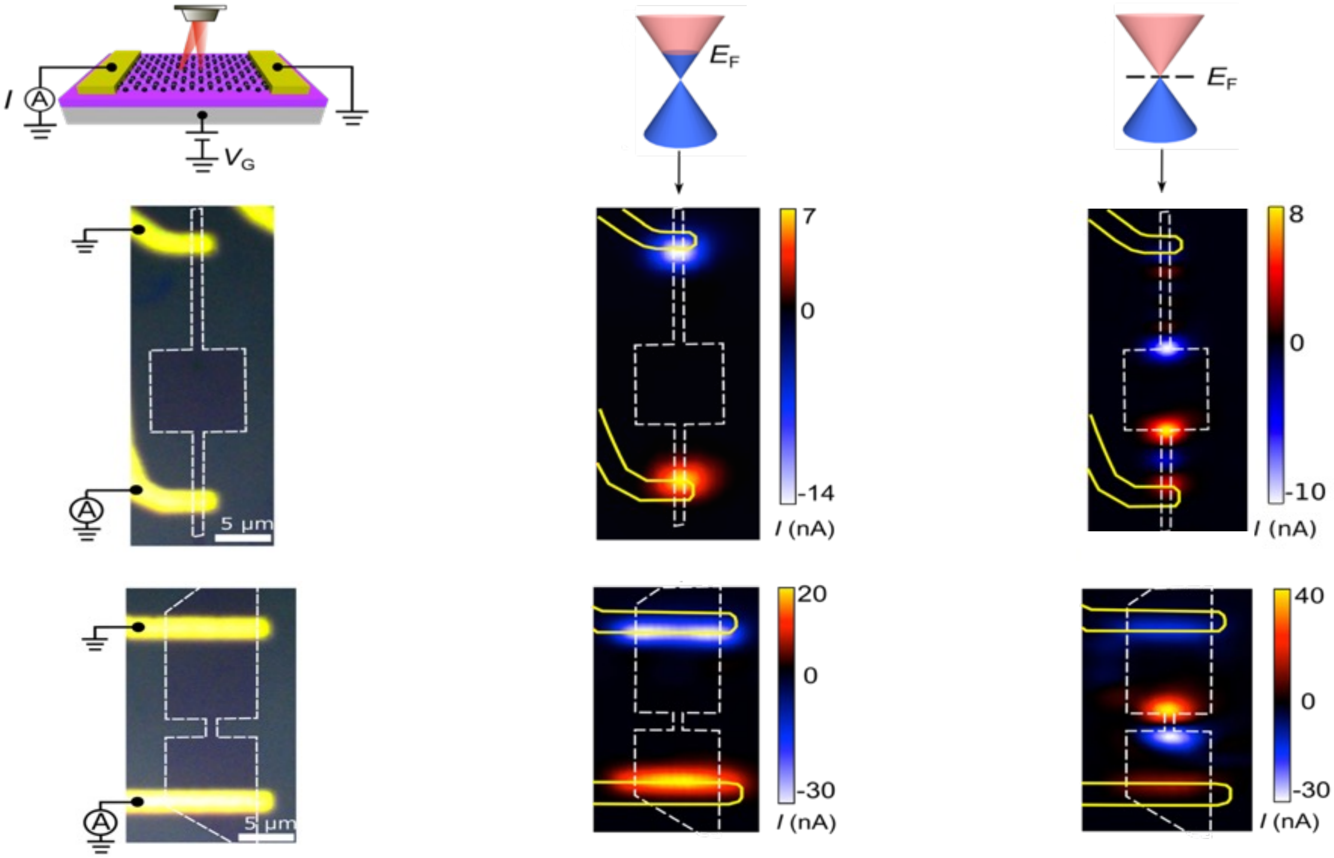

<u>**Ma**</u>, *et al.*, Nature Nano. (2019)

Outline

- Intrinsic photocurrents in WTe_2
- Intrinsic photocurrents in inversion-breaking Weyl
- Intrinsic photocurrents and emergent chirality
- Outlook

Topological Weyl semimetal

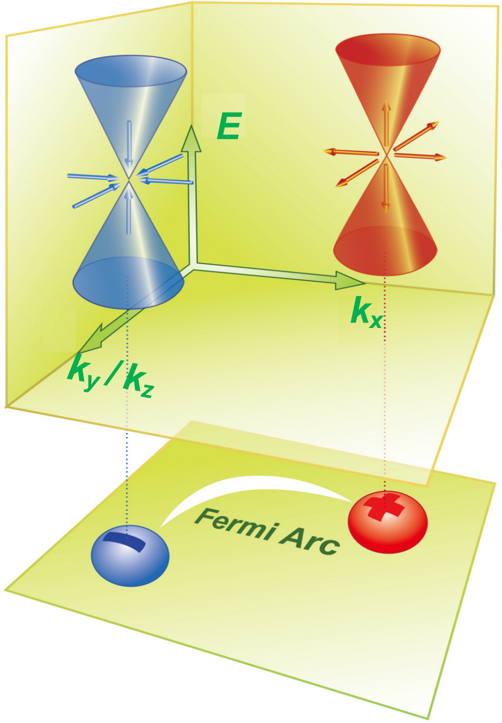

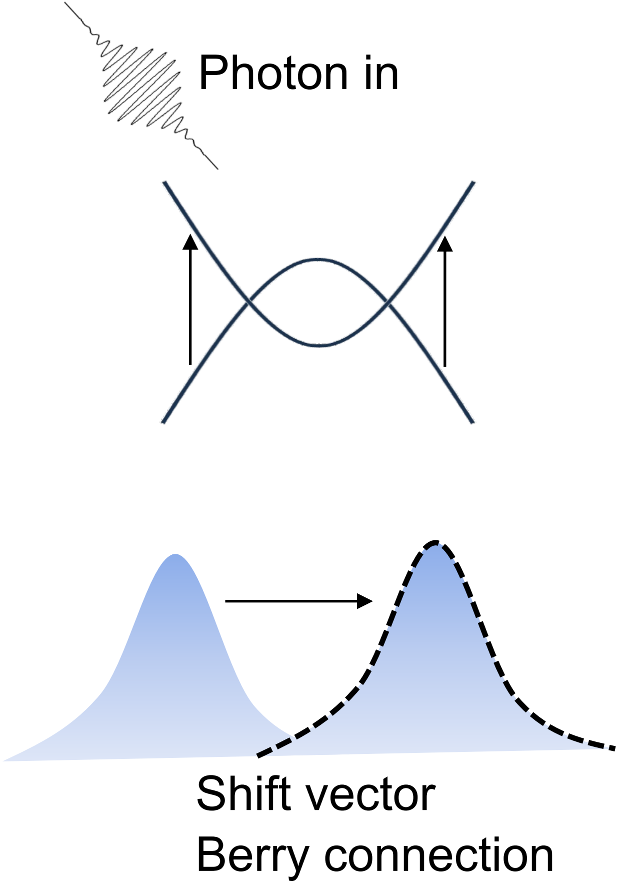

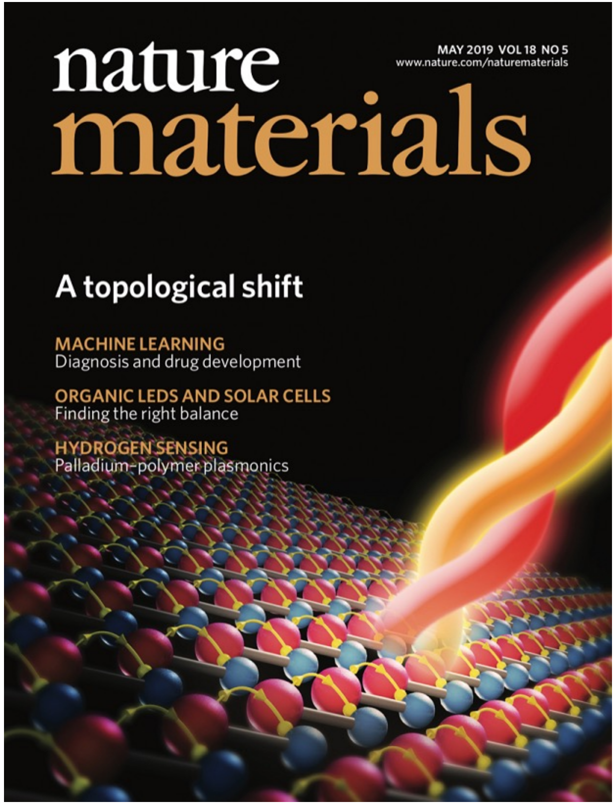

Shift current in Type I Weyl TaAs

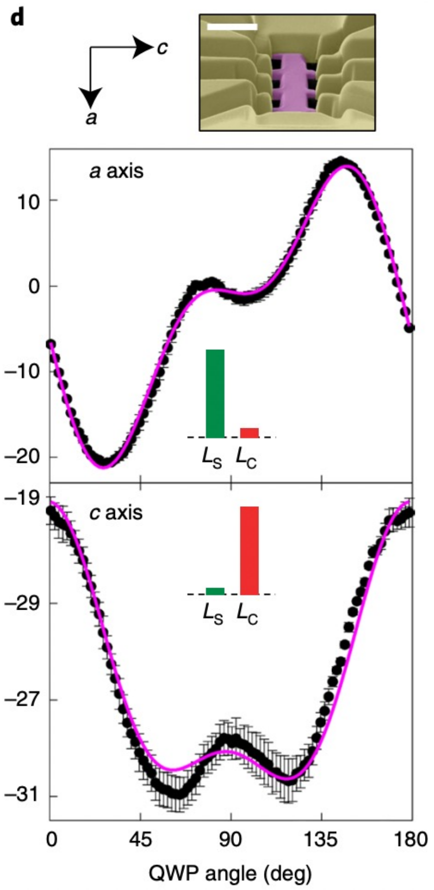

nature > nature materials > articles > article

Article | Published: 04 March 2019

Colossal mid-infrared bulk photovoltaic effect in a type-I Weyl semimetal

Gavin B. Osterhoudt, Laura K. Diebel, Mason J. Gray, Xu Yang, John Stanco, Xiangwei Huang, Bing Shen, Ni Ni, Philip J. W. Moll, Ying Ran & Kenneth S. Burch

Nature Materials **18**, 471–475 (2019) | Cite this article

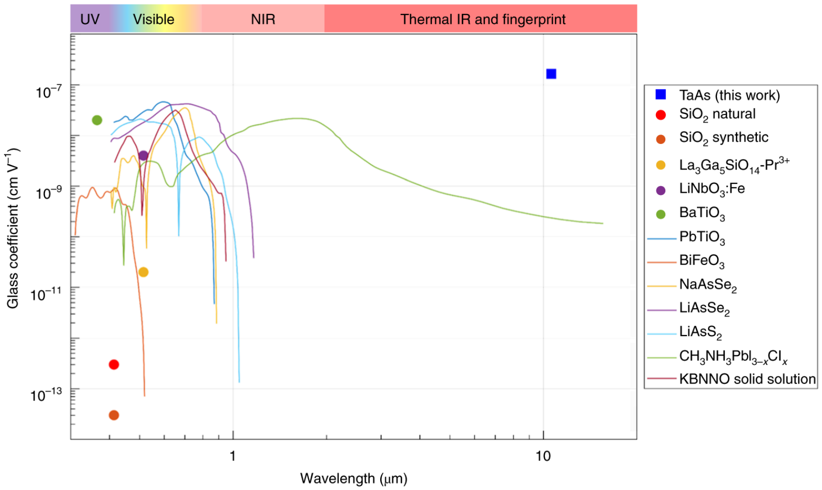

Shift current in Type II Weyl $TaIrTe_4$

nature > nature materials > articles > article

Article | Published: 04 March 2019

Nonlinear photoresponse of type-II Weyl semimetals

Junchao Ma, Qiangqiang Gu, Yinan Liu, Jiawei Lai, Peng Yu, Xiao Zhuo, Zheng Liu, Jian-Hao Chen, Ji Feng & Dong Sun

Nature Materials **18**, 476–481 (2019) | Cite this article

Approaching commercial low-temperature detectors

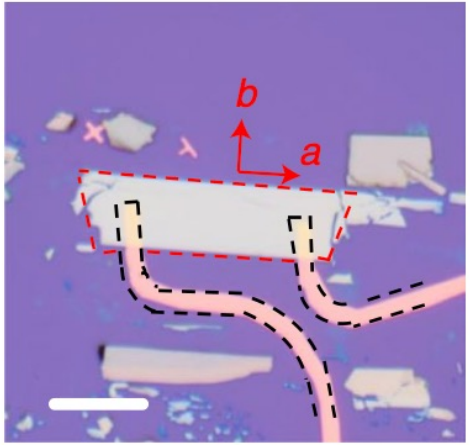

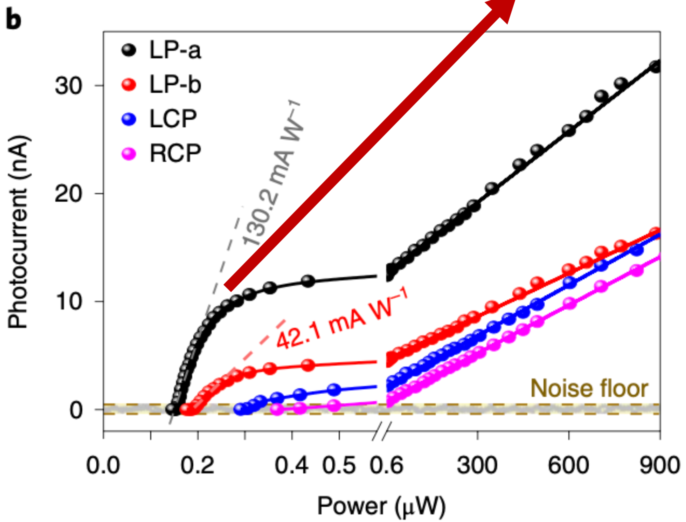

Chiral light and Chiral fermion

Circularly polarized light

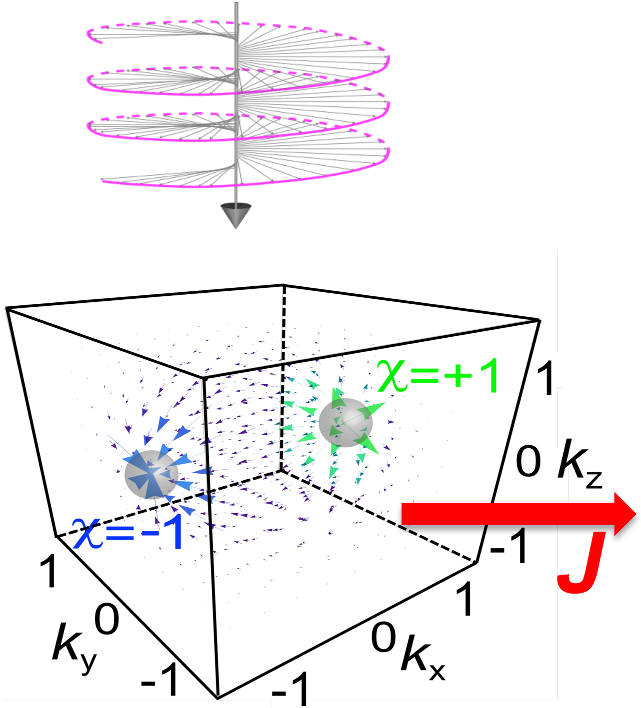

Chan et al. PRB **95**, 041104 (2017)

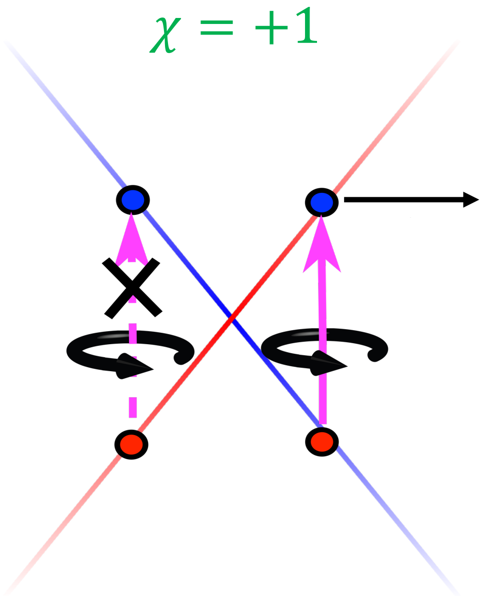

Berry curvature

$$|\mathcal{P}^{\mathrm{RCP}}(\vec{k})|^2 - |\mathcal{P}^{\mathrm{LCP}}(\vec{k})|^2 \propto \Omega(\vec{k})$$

Berry curvature (Chirality) selection rules in Weyl semimetals

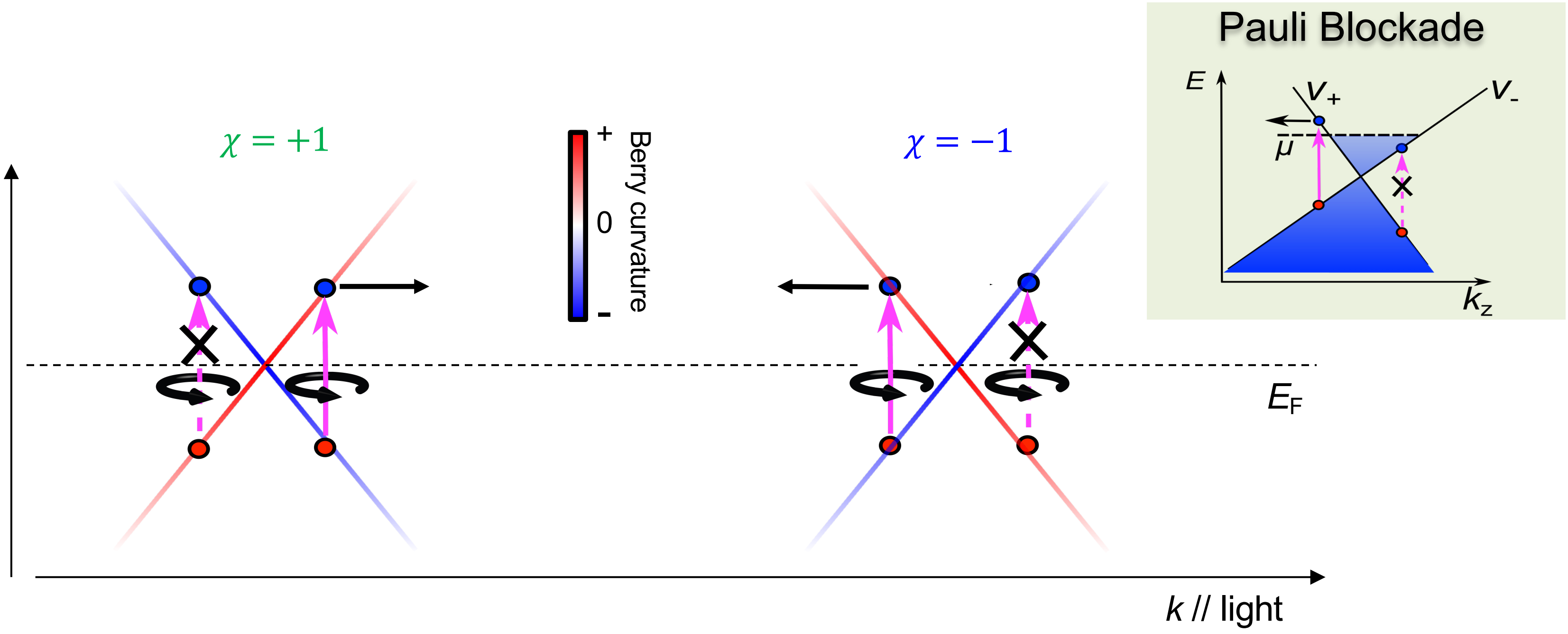

Cancellation can be lifted if the crystal symmetry allows the response.

A dramatic example will be shown.

Observation of CPGE in Weyl TaAs

TaAs

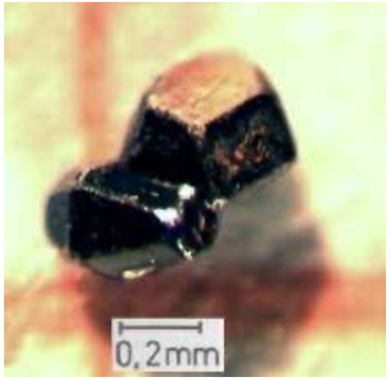

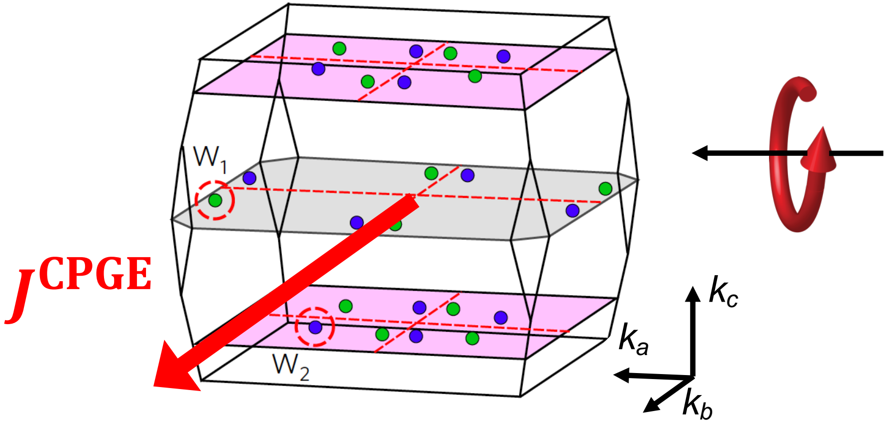

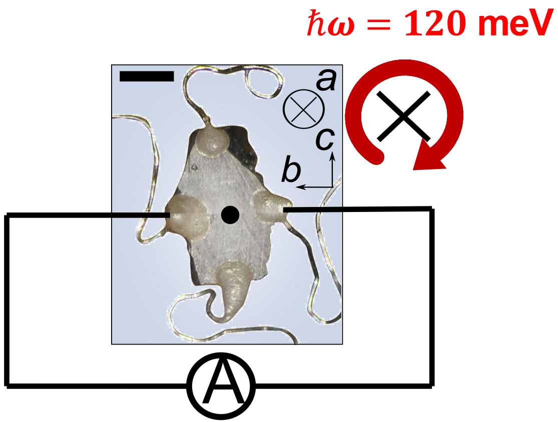

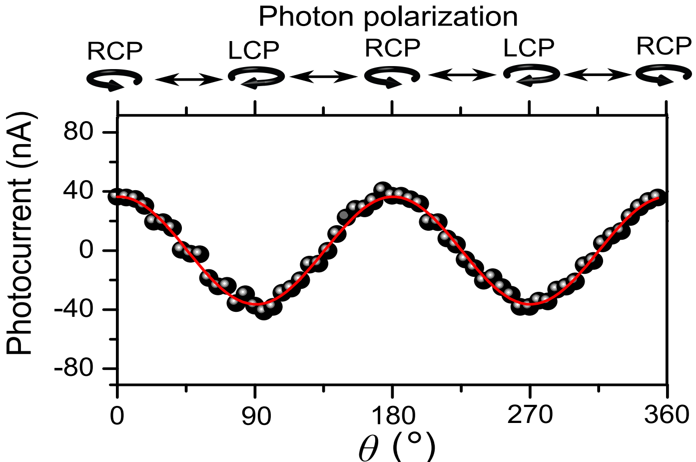

Ma, *et. al.*, **Nature Phys.** (2017)

A dramatic example of the effect of Pauli blocking

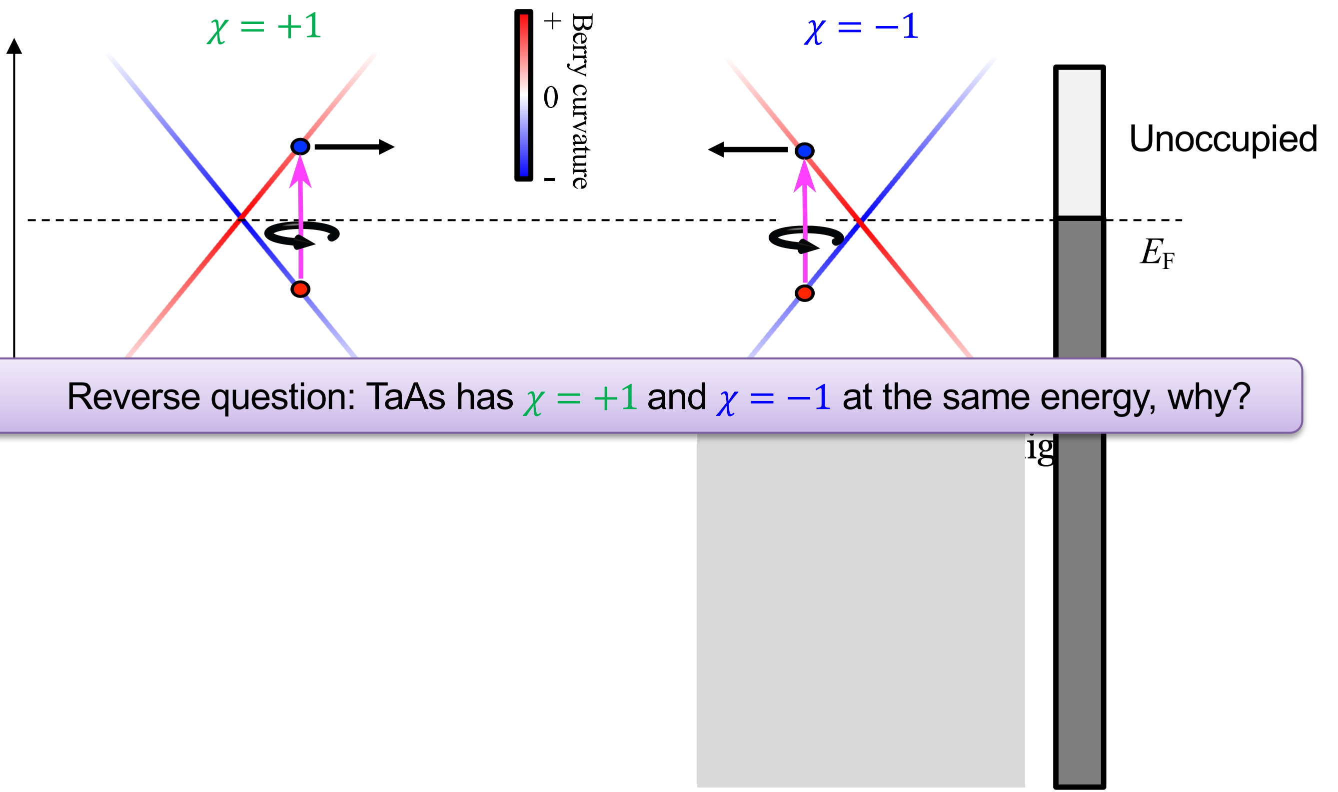

Reverse question: TaAs has $\chi = +1$ and $\chi = -1$ at the same energy, why?

Symmetry transformation of the chirality of Weyl nodes

Ta

As

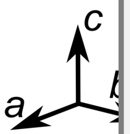

Symmetry		Effect on Weyl
Inversion	✗	Reverse χ
Mirror	✗	Reverse χ
Roto-inversion	✗	Reverse χ
Rotation	✓	Preserve χ
Time-reversal	✓	Preserve χ

With … ergy.

Topological chiral crystals

Chiral crystal

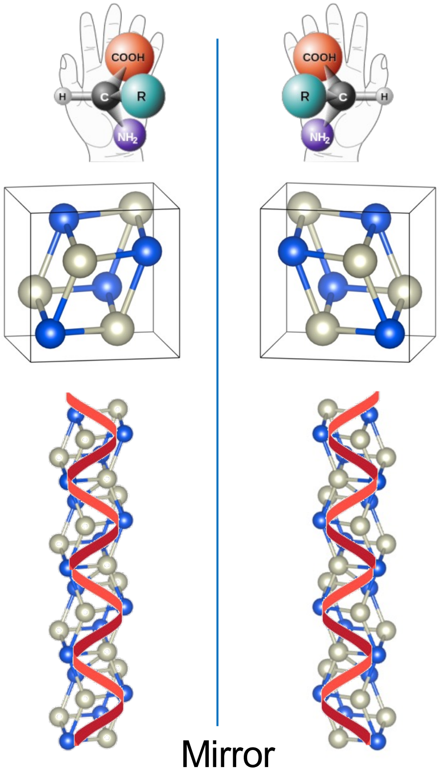

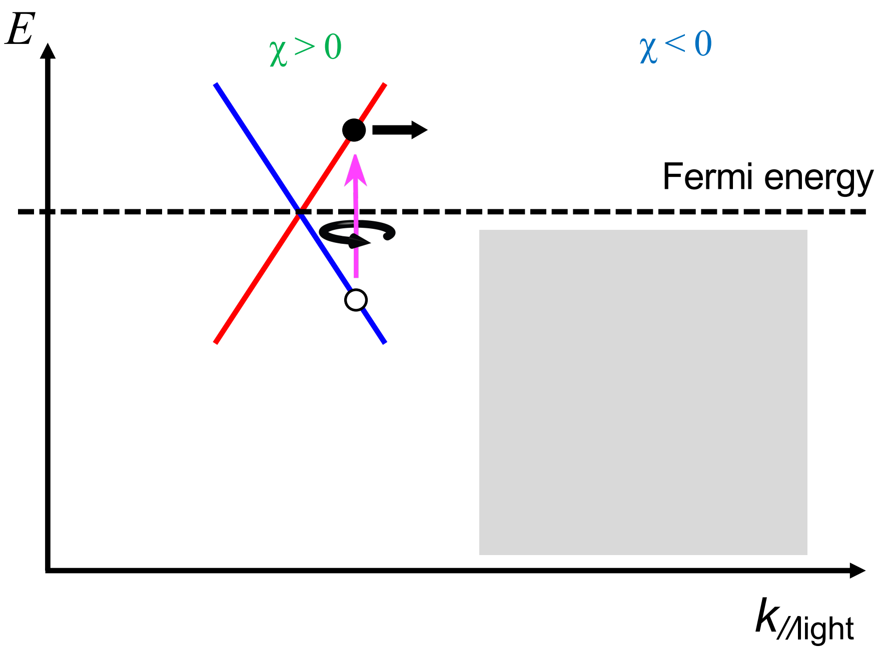

Quantized CPGE in topological chiral crystals

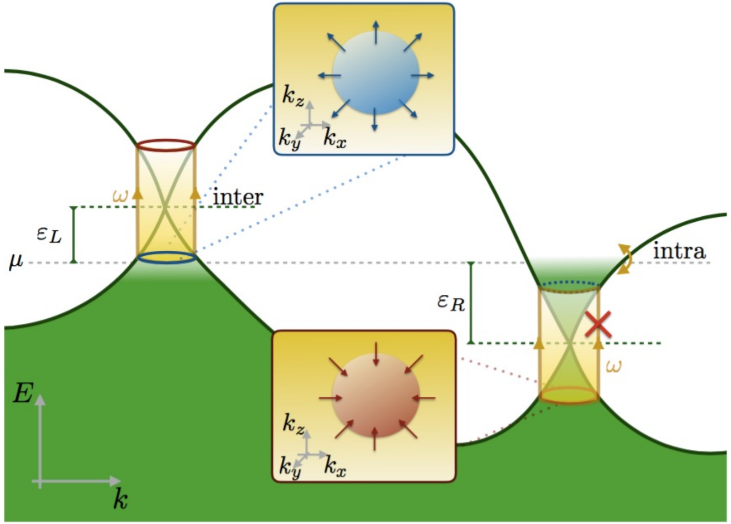

Open Access | Published: 06 July 2017

Quantized circular photogalvanic effect in Weyl semimetals

Fernando de Juan, Adolfo G. Grushin, Takahiro Morimoto & Joel E Moore

Nature Communications **8**, Article number: 15995 (2017) | Cite this article

Fine structure constant

$$\frac{1}{2}\left[\frac{dj_{\circlearrowright}}{dt} - \frac{dj_{\circlearrowleft}}{dt}\right] = \frac{2\pi e^3}{h^2 c\epsilon_0} I C_i = \frac{4\pi\alpha e}{h} I C_i$$

Light intensity

Topological charge

CPGE in topological chiral crystal RhSi and CoSi

Multifold chiral fermion crystal RhSi

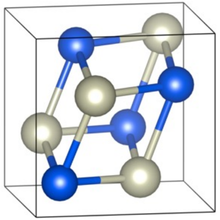

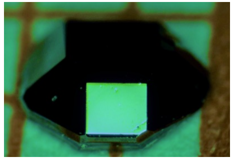

Theoretical computation
of quantized CPGE in RhSi

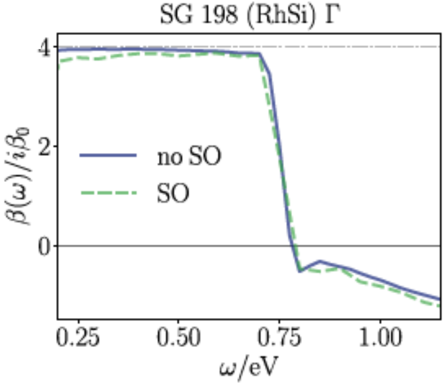

Flicker, *et. al.*, **PRB** (2018)

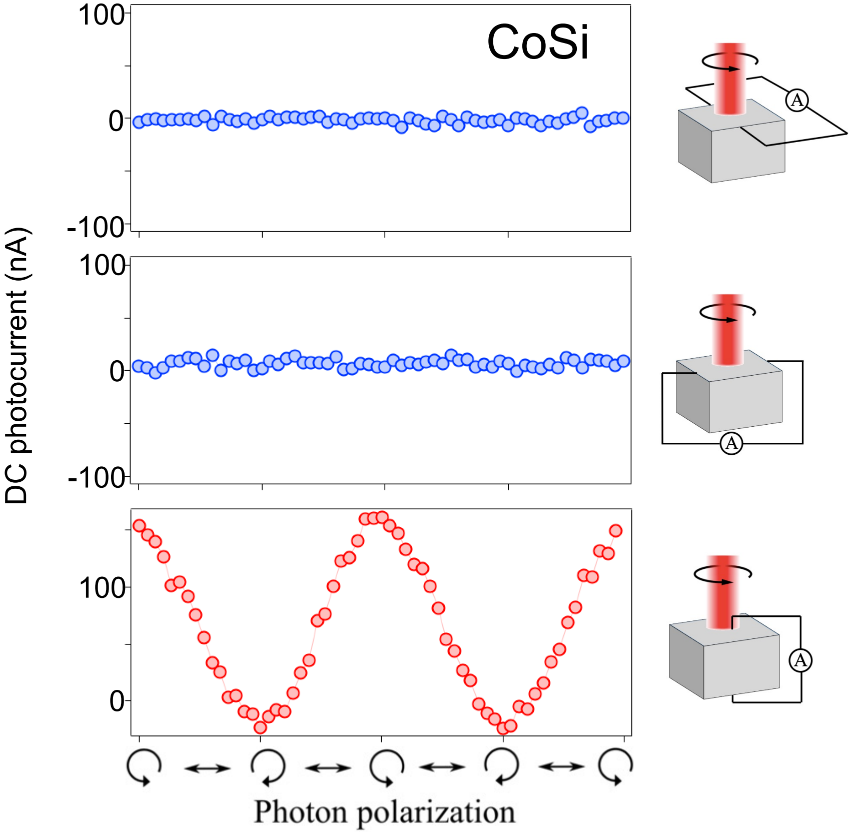

Quantized CPGE

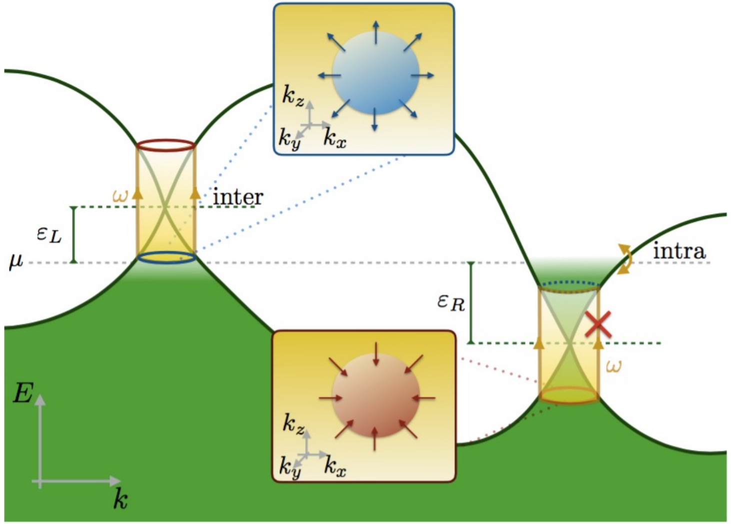

Open Access | Published: 06 July 2017

Quantized circular photogalvanic effect in Weyl semimetals

Fernando de Juan, Adolfo G. Grushin, Takahiro Morimoto & Joel E Moore

Nature Communications **8**, Article number: 15995 (2017) | Cite this article

$$\frac{1}{2}\left[\frac{dj_{\circlearrowright}}{dt} - \frac{dj_{\circlearrowleft}}{dt}\right] = \frac{2\pi e^3}{h^2 c\epsilon_0} I C_i = \frac{4\pi\alpha e}{h} I C_i$$

Current injection rate

Time-resolved measurements

Time-resolved photocurrent measurement - THz emission

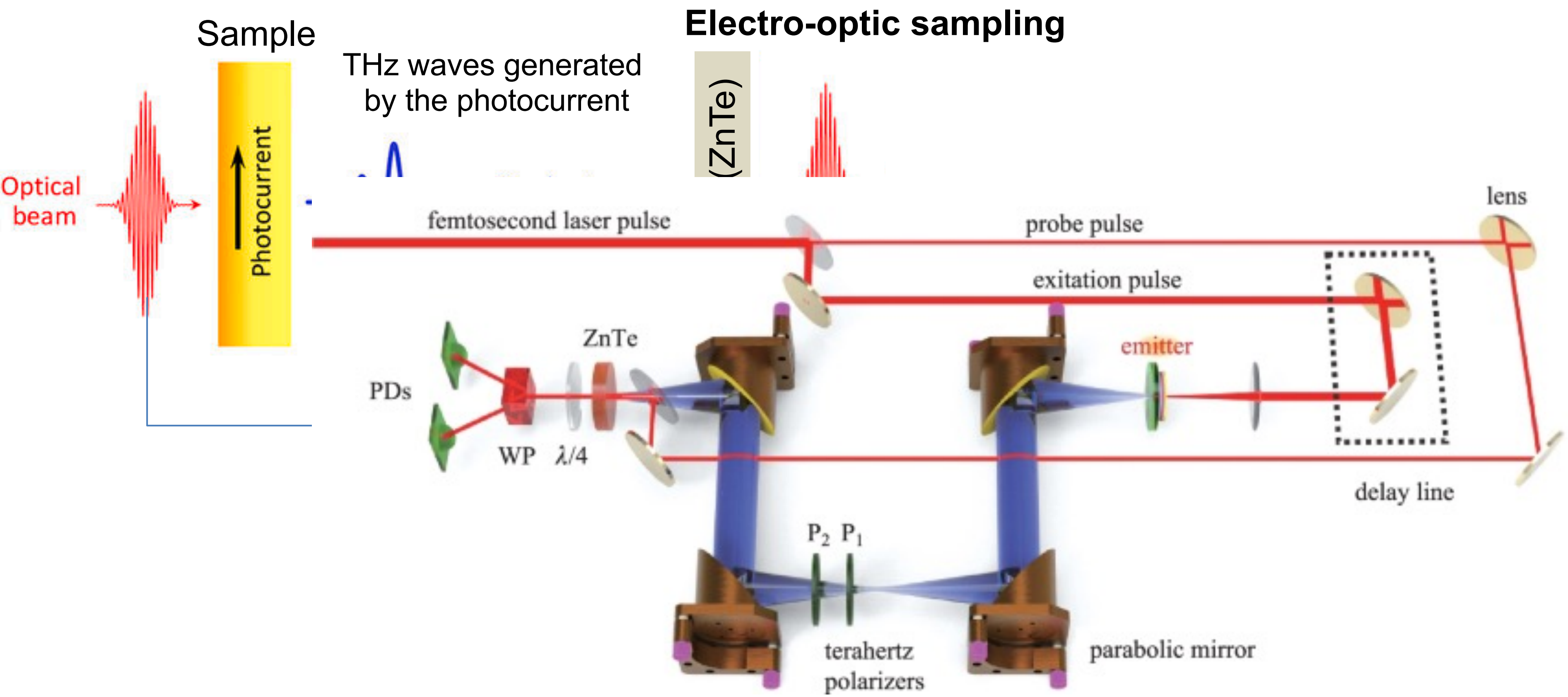

Front. Optoelectron. **15**, 12 (2022)

CPGE measured through THz emission in chiral fermions

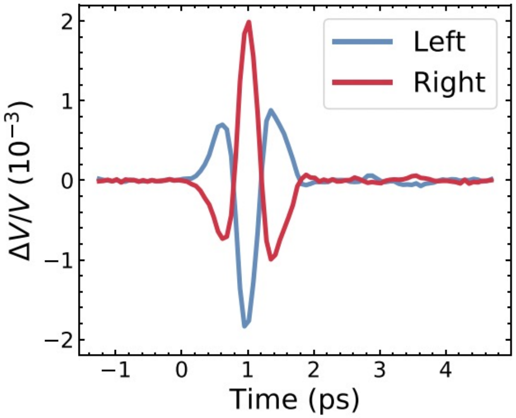

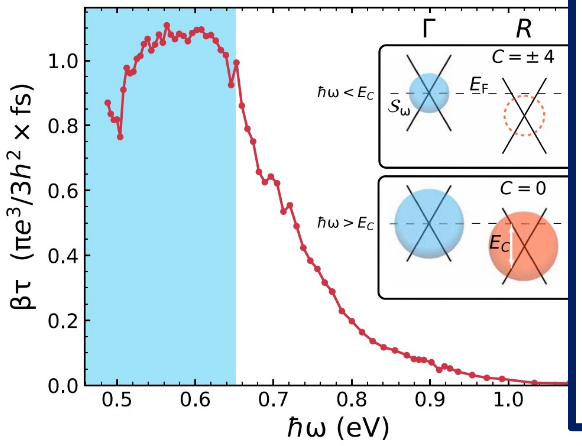

RESEARCH ARTICLE | OPTICS

Quasi-steady state

We note first that this amplitude is proportional to the βτ product, where τ is the momentum lifetime of photexcited carriers, rather than β itself. The reason is that the dynamics are in the quasi–steady state regime of Eq. 1, in which τ is shorter than the ~100-fs duration of the excitation pulse. This conclusion follows from the observation that the terahertz emission waveform follows the envelope of the laser pulse, rather than persisting for an observable momentum lifetime. The quasi–steady state regime is consistent with τ = 8 fs for equilibrium carriers as determined from transport measurements (see the Supplementary Materials). The τ of photoinjected "hot" carriers can be expected to be at least as short as that of the equilibrium ones.

Flicker, *et. al.*, PRB (2018)

Structure chirality controls the electronic chirality

Chiral crystal

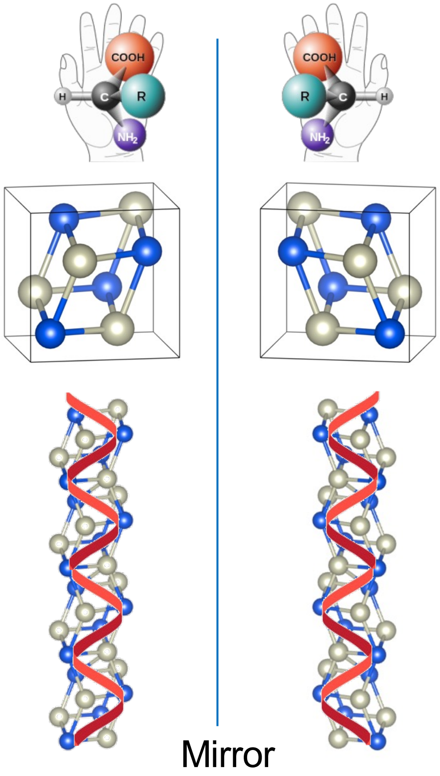

Left

Right

Left

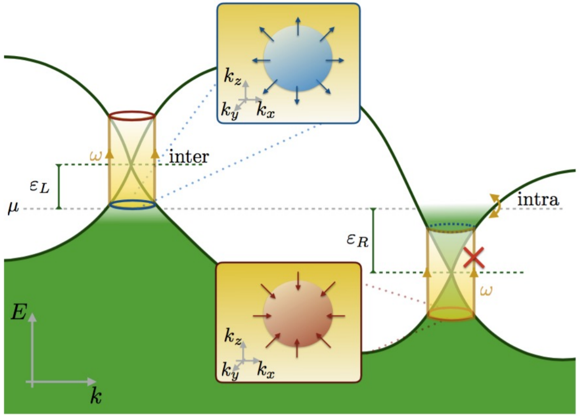

Right

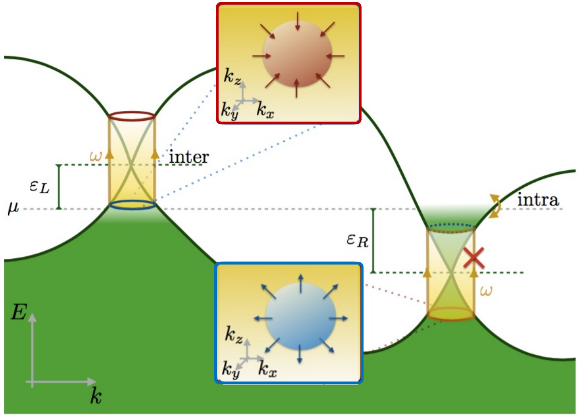

Outline

- Intrinsic photocurrents in WTe_2
- Intrinsic photocurrents in inversion-breaking Weyl
- Intrinsic photocurrents and emergent chirality
- Outlook

Chiral charge density wave

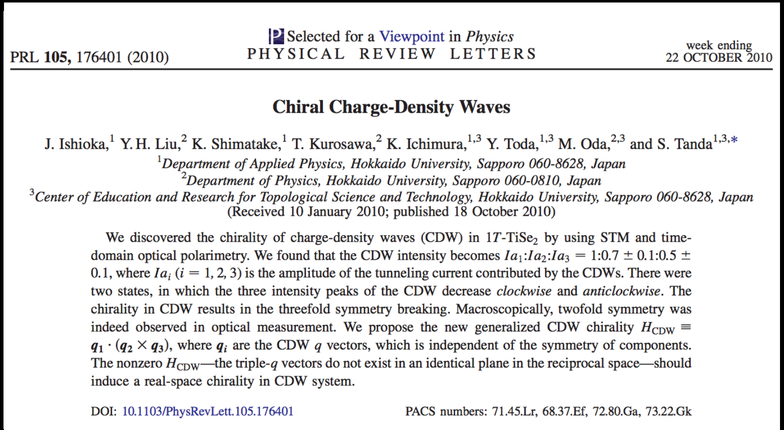
PRL **105**, 176401 (2010) Selected for a Viewpoint in *Physics* PHYSICAL REVIEW LETTERS week ending 22 OCTOBER 2010

Chiral Charge-Density Waves

J. Ishioka,[1] Y. H. Liu,[2] K. Shimatake,[1] T. Kurosawa,[2] K. Ichimura,[1,3] Y. Toda,[1,3] M. Oda,[2,3] and S. Tanda[1,3,*]

[1]*Department of Applied Physics, Hokkaido University, Sapporo 060-8628, Japan*
[2]*Department of Physics, Hokkaido University, Sapporo 060-0810, Japan*
[3]*Center of Education and Research for Topological Science and Technology, Hokkaido University, Sapporo 060-8628, Japan*
(Received 10 January 2010; published 18 October 2010)

We discovered the chirality of charge-density waves (CDW) in 1*T*-$TiSe_2$ by using STM and time-domain optical polarimetry. We found that the CDW intensity becomes $Ia_1{:}Ia_2{:}Ia_3 = 1{:}0.7 \pm 0.1{:}0.5 \pm 0.1$, where Ia_i ($i = 1, 2, 3$) is the amplitude of the tunneling current contributed by the CDWs. There were two states, in which the three intensity peaks of the CDW decrease *clockwise* and *anticlockwise*. The chirality in CDW results in the threefold symmetry breaking. Macroscopically, twofold symmetry was indeed observed in optical measurement. We propose the new generalized CDW chirality $H_{CDW} \equiv \boldsymbol{q}_1 \cdot (\boldsymbol{q}_2 \times \boldsymbol{q}_3)$, where $\boldsymbol{q}_i$ are the CDW q vectors, which is independent of the symmetry of components. The nonzero H_{CDW}—the triple-q vectors do not exist in an identical plane in the reciprocal space—should induce a real-space chirality in CDW system.

DOI: 10.1103/PhysRevLett.105.176401 PACS numbers: 71.45.Lr, 68.37.Ef, 72.80.Ga, 73.22.Gk

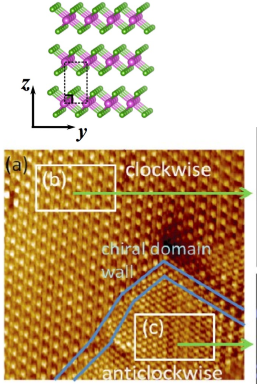

Correlated semimetal $TiSe_2$

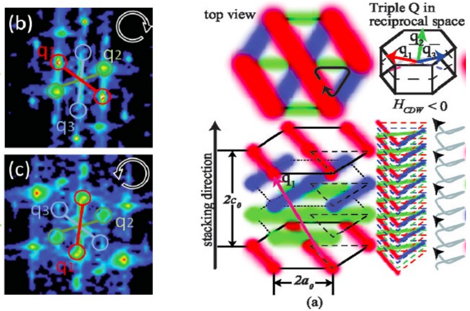

Kagome correlated metal KV_3Sb_5

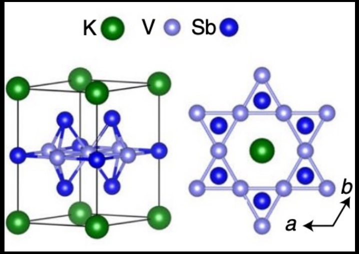

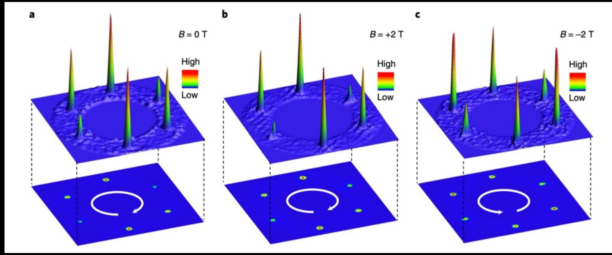

J. Yin, et al., Nature Materials 20, 1353 (2021)

Quantum spin liquid 1T-TaS_2

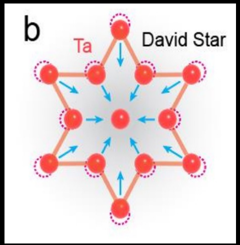

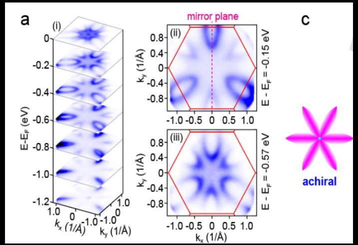

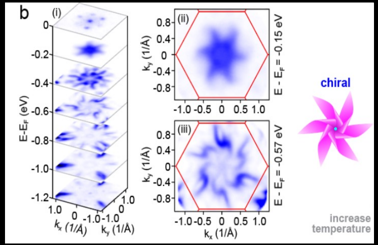

H. Fang, et al., Phys. Rev. Lett. 129, 156401 (2022)

Our approach: nonlinear photocurrent

Longitudinal CPGE

CPGE current generated along the light propagation direction

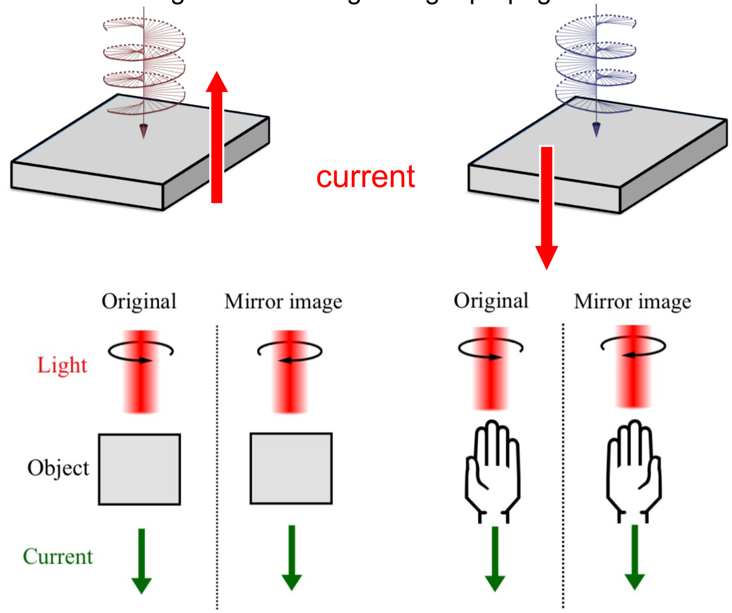

Longitudinal CPGE ⇄ Material chirality

Chiral crystal CoSi

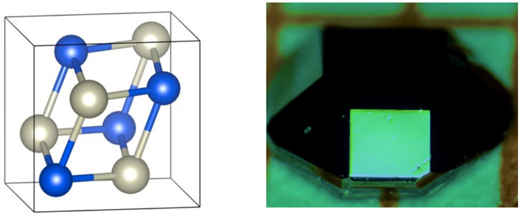

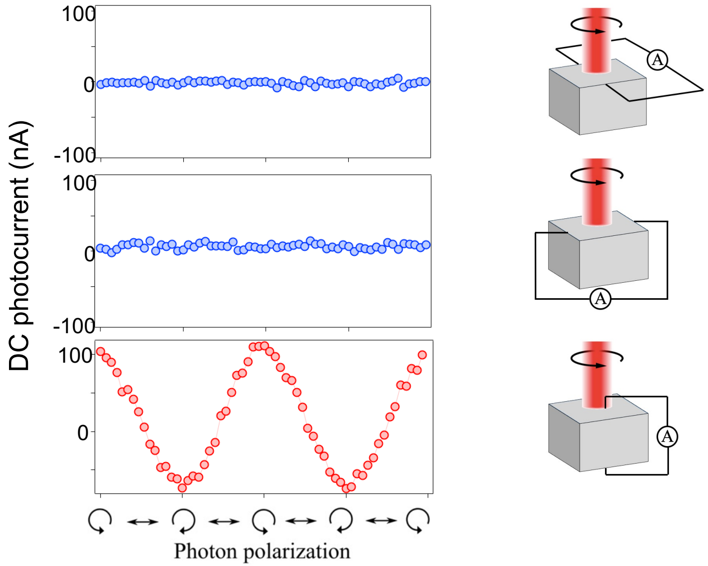

Ma *et. al.*, unpublished

No CPGE during dark cooling

250 K

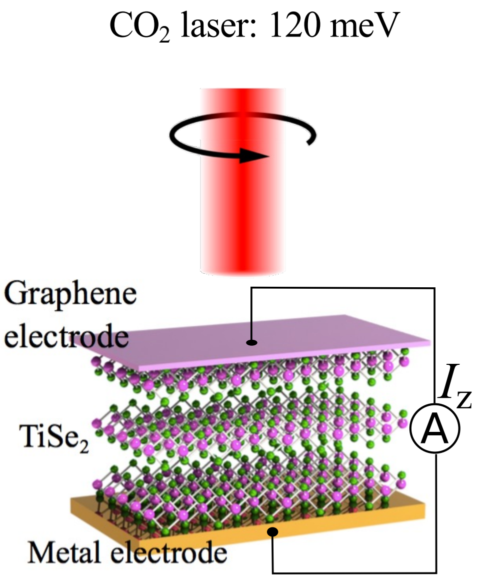

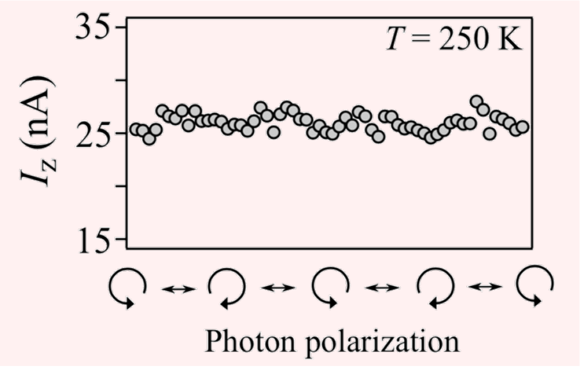

No CPGE during dark cooling

250 K

↓

50 K

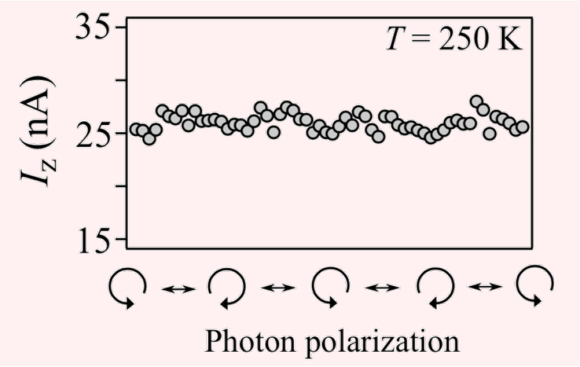

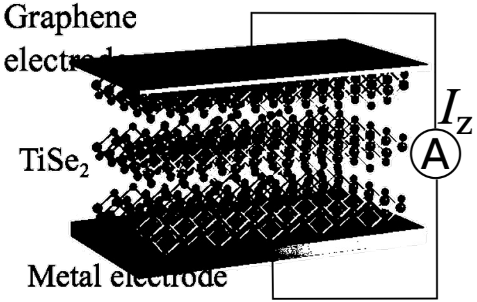

No CPGE during dark cooling

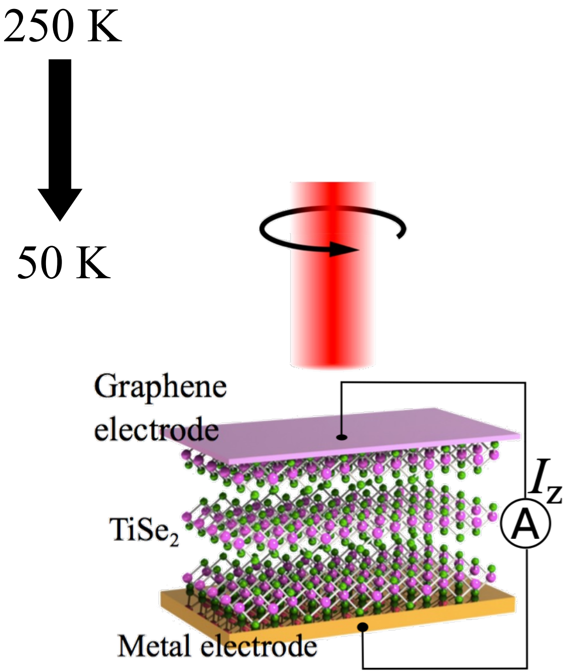

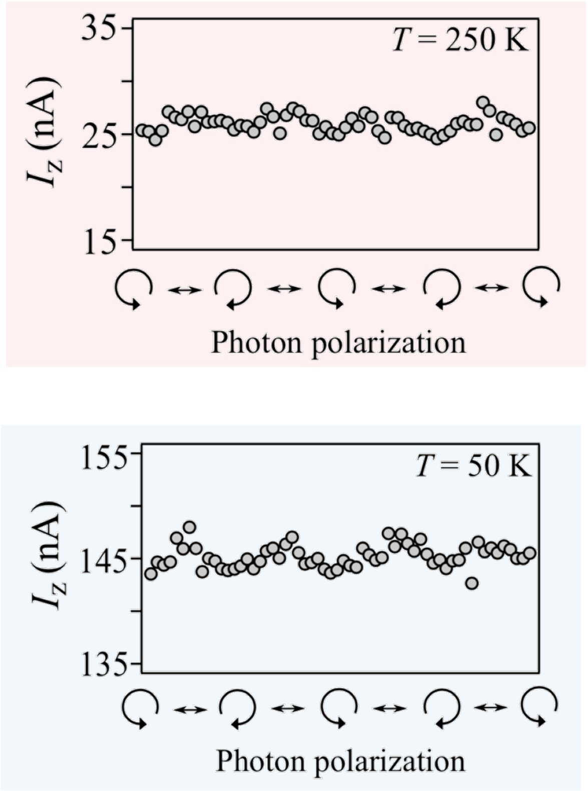

- No chiral phase
- Technique not sensitive enough
- **Signal averaged out by domains of opposite chirality**

Large CPGE after optical training/induction

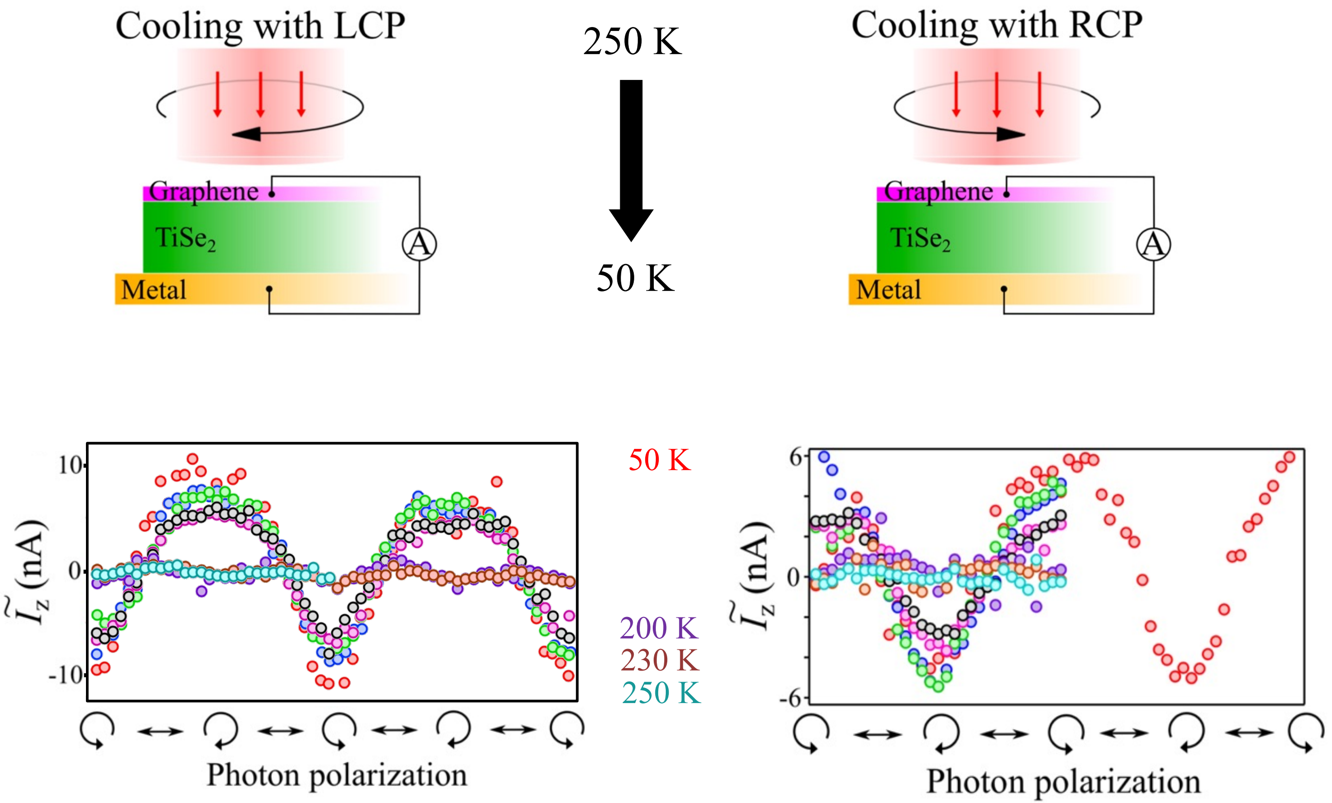

Nature 578, 545 (2020)

Large CPGE after optical training/induction

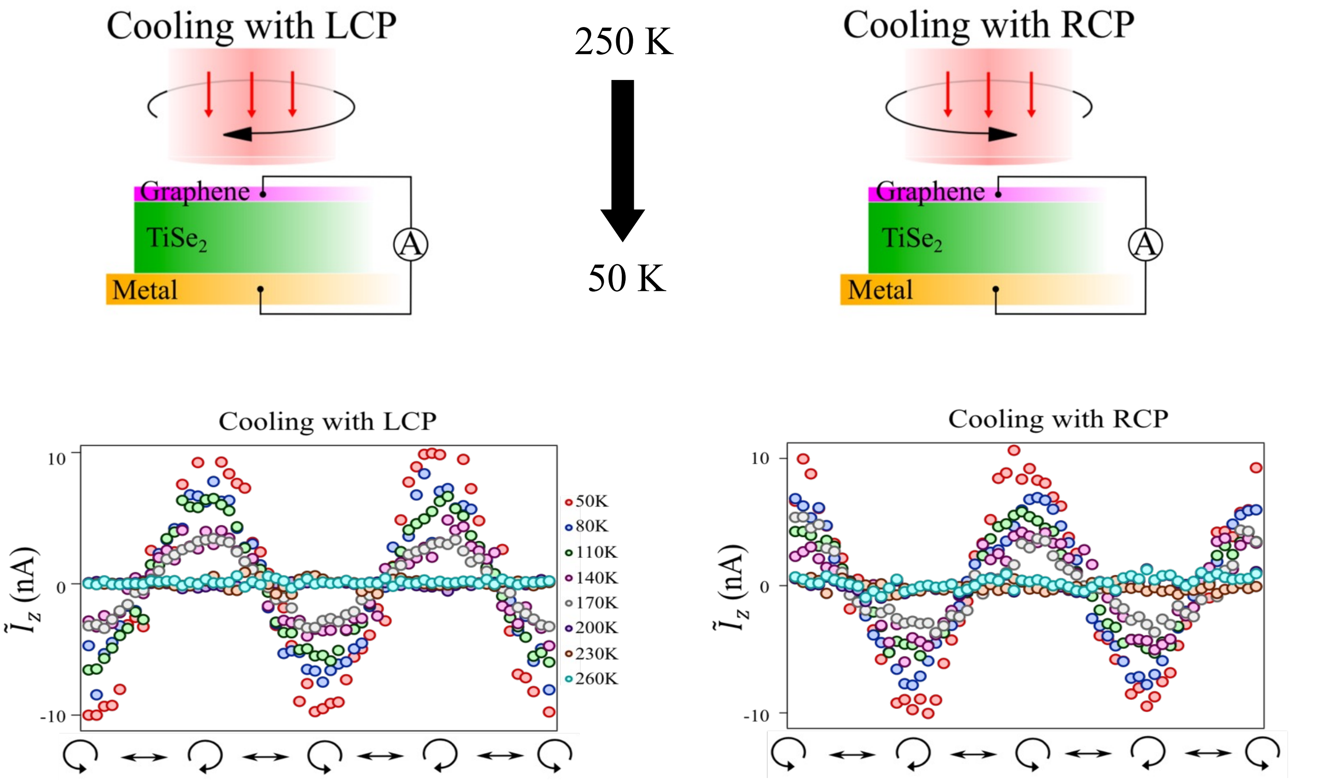

Photon energy dependence of the training and detection

Training

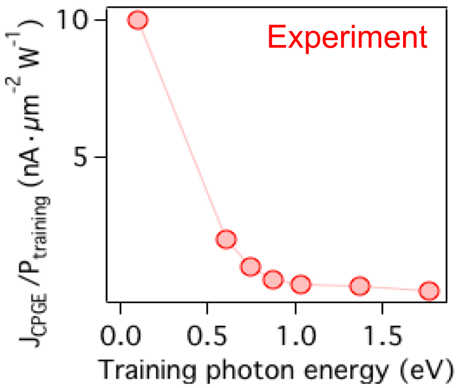

Detection

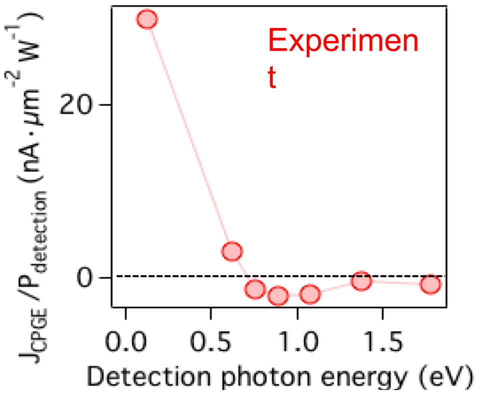

PRB 99, 155103 (2019)

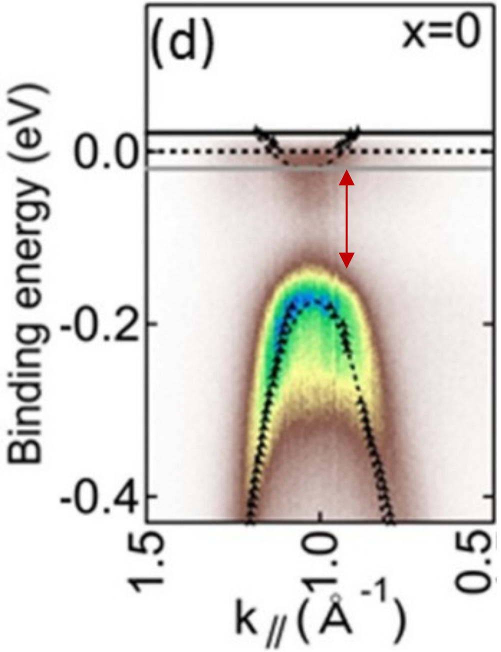

Outline

- Intrinsic photocurrents in WTe_2
- Intrinsic photocurrents in inversion-breaking Weyl
- Intrinsic photocurrents and emergent chirality
- Outlook

magneto-photocurrents

Charge photocurrent	Circular injection	Linear shift	Circular shift	Linear injection
P symmetry	×	×	×	×
T symmetry	✓	✓	×	×
PT symmetry	×	×	✓	✓
Material examples	TaAs, CoSi, RhSi, Td-W(Mo)Te_2	TaAs, CoSi, RhSi, Td-W(Mo)Te_2	Even-layered $MnBi_2Te_4$ Even-layered CrI_3	Even-layered $MnBi_2Te_4$ Even-layered CrI_3
Microscopic process	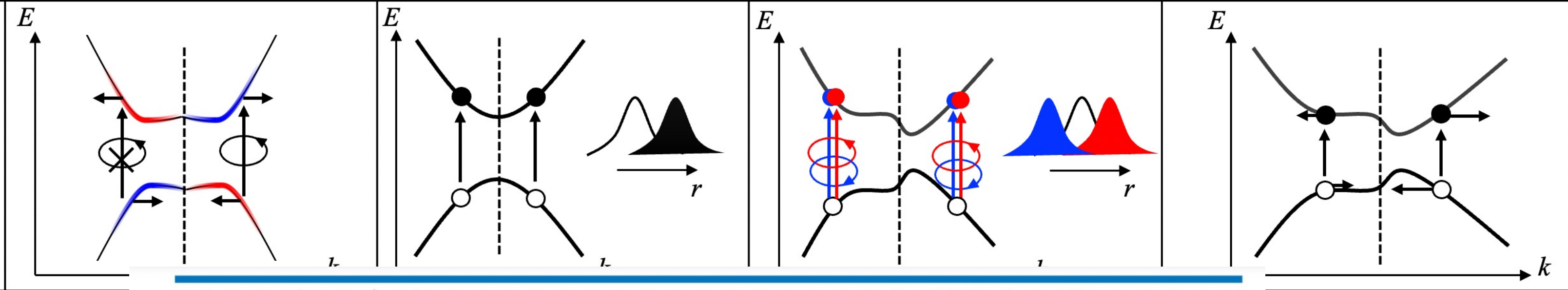			
Geometric quantity	Berr			Quantum metric (dipole)

nature reviews physics

https://doi.org/10.1038/s42254-022-00551-2

Technical review

Check for updates

Photocurrent as a multiphysics diagnostic of quantum materials

Qiong Ma[1,2], Roshan Krishna Kumar[3], Su-Yang Xu[4], Frank H. L. Koppens[3,5] & Justin C. W. Song[6]